Annals of R.S.C.B., ISSN: 1583-6258, Vol. 25, Issue 7, 2021, Pages. 1473 – 1488
Received 05 May 2021; Accepted 01 June 2021.

An Effective Photocatalyticdegradation of Rose Bengal and Eosin Y by Using ZnO Nanoparticles as a Photocatalysts

TajneesPirzada*, FayazHussainKanhar, Mir Munsif Ali Talpur, Weenghar Ali Chandio, ZulfiqarJumani, Imran Ali Chandio
Institute of Chemistry, Shah Abdul Latif University, Khairpur 66020, Sindh, Pakistan.
Corresponding Email: tajnees@yahoo.com

Abstract

Environmental contamination is the major challenging issue for the advanced and upgrowing countries due to exceptional industrial development. Dyes have played a vital role in global pollution if they are not treated appropriately. In this study heterogeneous photocatalysis process,well-known semiconductor, ZnO nanoparticles (ZnONPs) are used for the degradation of dyesdue to its capability to take part in both acid-base and redox reaction. Precipitation is a highlyeffective and recognized method used to synthesize ZnO NPs, were successfully synthesized and characterized by applying various spectroscopic techniques i.e. XRD, SEM, AFM, ZP, FT-IR, and UV-Visible. Engineered nanoparticles were applied to check their effectiveness on the photocatalytic reduction of dyes, Rose Bengal (RB), and Eosin Y (EY) dyes in the aqueous medium. The catalyst showedpotential photocatalytic efficiency up to 98% RB using 300 µg and >95% EY using 350 µg at 7pH. Dyes degraded completely within 3 minutes under sunlight at maximum absorbance value (λ max) 548and 515 nm, respectively. Moreover, various factors were optimized during degradation protocoli.e. sunlight, irradiation time, reducing agent, power of hydrogen, dyes concentration, and catalyticdose. The elevatedphotocatalyticdegradation efficiencyof both dyes (RB and EY up to 98% wereobserved. Consequentially, the dyes reported in this study specially EY has never been tested before with pure ZnOnanocatalyst hence ZnO NPs can be suggested as a more effectivephotocatalyst for thesuccessful degradation of complex dyes then reported due to their complex structureat the commercial level.

Keywords; Precipitation method, Photocatalytic degradation, Pollution, Rose Bengal, Eosin Y, ZnONanocatalyst, Sunlight.

Graphical Abstract

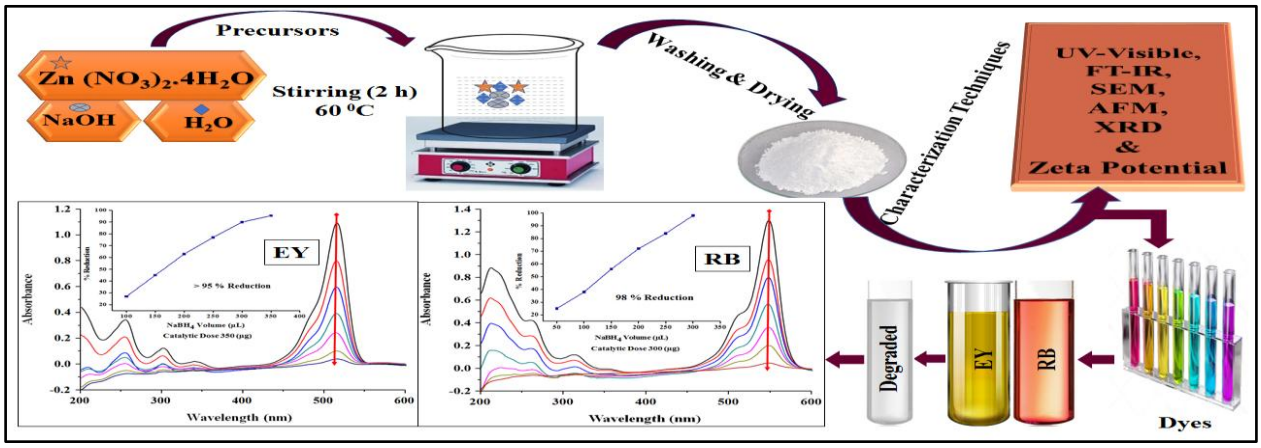

Figure. 1: Graphical representation of synthesis and degradation of RB and EY.

Annals of R.S.C.B., ISSN: 1583-6258, Vol. 25, Issue 7, 2021, Pages. 1473 – 1488
Received 05 May 2021; Accepted 01 June 2021.

1. Introduction

In the industrial wastewater, color is the major pollutant, extremely visible that affecting the visual quality, transparency, and gas solubilities of water bodies due to the intermixing of very low quantity of synthetic dyes (< 1 ppm) in water. Dyes have curious effects on the aquatic life and deferring of photosynthesis depends upon their concentration due to the reflection and absorption of the sunlight entering in water.So, the process of degradation of dyes from wastewater is not only to remove color but alsodecreases toxicity simultaneously[1].Mostly in all the industries, organic dyes are used like rubber, cosmetics, drugs, food, paints, and textile industries and continuously released in the atmosphere and water bodies hence organic dyes are highly toxic for the environment if they are not treated properly[2].

The most supreme contaminated variety of wastewater is the dyes, containing high pH, (COD) chemical oxygen demand, and low degradability, having a severe effect when not disposed of well[3].The amount of dye effluent which is released in the high quantity by the textile industries is highly dangerous for the aquatic life ecosystem as well as for human beings[4].It is very difficult to decompose their anaerobic degradation effect incarcinogenic products under natural conditions because of water stable and structure containing compounds. Therefore, the major requirement is the removal or degradation of toxic components into non-toxic components[5].In the previous few years, there are serval resources have been used to treat dyes existing in the wastewaters as well as the conventional biological and chemical methods, but not effective to remove the toxicity of dyes in wastewater[6].Many methods are selected for the treatment of wastewater such as membrane filtration, ion exchange, and coagulation-flocculation processes, etc.[7], but on a small scale, these are not apocopate for industries due to high resources and recurring expenditures. Therefore, metal oxide semiconductors photocatalyst by the Advanced Oxidation Process (AOP) have been grown much attention over old processes because of its simplicity and quick oxidation[8].

In the process of AOP, there is an ultraviolet, infrared or visible light is used for the fragmentation of dyes molecules in the availability of the photocatalyst and there are many heterogeneous photocatalyst semiconducting materials such as ZnO, TiO_2 and Fe_2O_3, etc. were used for various dyes treatment due to their capacity to contribute in both acid-base and redox reaction[9].However, the adsorption process is found to be a very cheap, effective,and interesting photocatalyst nowadays[10]due to its potential uses in the various areascontaining energy, catalysis, and atmospheric issues[11].But in the existence of UV light,most of these catalystsare active[12].There is a lot of effortthat has been completed in the earlier to improve sensitivity, activity, and good absorption of visible light[13],and these have many benefits for their low cost and no need for pressure or temperature for the degradation of dyes. Therefore, the photocatalystis improved on more emerging new methods to reduce the combination of water contaminants and many dyes, etc. from the industrial wastage and domestic wastewater[14].These photocatalysts were used for the degradation without any making ofminorimpurities and carry toend products having no toxicity[15]and these photocatalysts can also be separate able and reusable for the degradation or reduction[16].

The organic compound with anionic, water-soluble, photosensitive, odorless, and dark pink powder is used in the photochemical and textile industries broadly dyes namely RB ($C_{20}H_2C_{l4}I_4Na_2O_5$) is a dangerous for the skin (itching and blistering irritation) and corneal epithelium lead to eye redness, inflammation of the human's[17],while EY ($C_{20}H_6Br_4Na_2O_5$) is used in the paper and textile industries arewater-soluble dye and highly dangerous for irritation of the skin, pain, eye redness and

Annals of R.S.C.B., ISSN: 1583-6258, Vol. 25, Issue 7, 2021, Pages. 1473 – 1488
Received 05 May 2021; Accepted 01 June 2021.

permanently injured to the cornea because of damage of retinal ganglion cells of the human beings[18].There are so many dangerous effects of the inhalation of toxic dyes on the human organs such as failure of the liver, kidneys, damages of DNA in the gastrointestinal, dropping of the respiratory gas exchange ability due to that metabolites are contaminated and carcinogenic for life[19].

Transition metal oxides specially ZnO NPs are considered as one of the potential agents for the degradation of toxins (dyes) from wastewater, having greater degradation ability for organic dyes in water[20].Thereare so many benefits including low cost, low solubility in water, easy to synthesis and do not produce as a minor contaminant[21]. The novelty of this study is that the proposed nanocatalyst are practicallyapplied for the degradation of dyes specially EY and RB.The results proved that ZnO NPs are anexcellentcandidate for the degradation of the dyes speciallycomplexed structured dyes like EY and RB.

2. Experimental Work

2.1. Washing of Glasswares

The well-cleaned glasswares were used in the whole practical work, washed with a washing agent, and sonicated by using the presence of HNO_3(1%) for 5 minutes, rinsed carefully with milli-q water, and completelyget dry with the help of an oven.

2.2. Chemical and Reagents

Precursors like zinc nitrate tetrahydrate(Zn $(NO_3)_2.4H_2O$), sodium hydroxide (NaOH), milli-q water, and ($NaBH_4$) sodiumborohydride were used for synthetic protocols. RB and EY are ideal dyes for degradation when ZnO NPs were used as a catalyst. All the substances and componentswere used without any further purification and were of analytical grade.

2.3. Synthesis of ZnO NPs

A highly effective and well-recognized precipitation scheme was used to prepareZnO NPs. In the typical procedure (Zn $(NO_3)_2.4H_2O$) (2 g) were dissolved in milli-q water (120 mL), stirred up to fully dissolved by using a magnetic stirrer, subsequently, 80 mL of NaOH having 0.5 M solution was added dropwise, until and unless the appearance of white color was observed and again continuously stirred at 60 ^{0}C for 2 hours then allowed to settle down nanoparticles for the whole night, later on, the supernatant was carefully discarded and remain white chalky solution got to dry at atmospherictemperature for 1 hour after dried in an oven at 95 ^{0}C for 2 hours and grinned samples were calcined at 450 ^{0}C for 2 hours in the furnace. Conclusively, the white precipitate of ZnO NPs gained was kept for advanced characterization and applied for the degradation of dyes.

2.4. Instrumentation

The morphological and topographical studies of synthesized ZnO NPs were examined by using SEM (JSM 6380 of Joel, Japan), AFM (AFM 5500 Agilent, USA) recorded a room temperature in which nanometric size and 3-D topography were revealed. The crystalline phase of ZnO NPs was manifested via XRD in which (Bruker D8) with Cu Kα irradiation (λ = 1.54060 Å) was used. The surface charge on the particles in the medium was determined by using zeta potential (Malvern). FT-IR (Thermo Nicolet 5700) was used to know the functionalities in the nanoparticles at the range of 4000-500 cm^{-1} and the UV-Visible spectrophotometer model (UV 1800 SHIMADZU) was used at the range of 200-600 nm throughout the experiment.

Annals of R.S.C.B., ISSN: 1583-6258, Vol. 25, Issue 7, 2021, Pages. 1473 – 1488
Received 05 May 2021; Accepted 01 June 2021.

2.5. Catalytic Degradation of Dyes

The catalytic measurement of projected nanoparticles was evaluated by using RB and EY dyes. First 100 mL stock solution was prepared to have various concentrations i.e. 60, 50, 40, 30, 20, and 10 ppm then 50 µL of $NaBH_4$ (0.05 M) and 100 µg of ZnO NPs were taken in an appropriate volume of dye, sonicated for 30 seconds and kept under sunlight, lastly UV-Visible spectrophotometer was employed to check the degradation at a regular time of intervals. The % degradation efficiency was determined by the following formula.

$$\% \text{ Degradation } = \text{Xi} - \frac{\text{Xf}}{\text{Xi}} \times 100 \qquad (1)$$

Whereas X_i and X_f are initial and final absorbance of dyes, respectively.Moreover, asimilar protocol was followed for remaining factors such as the effect of pH, the effect of sunlight irradiation time, the effect of dye concentration, the effect of catalyst dose, and reducing agent[22].

3. Results and Discussion

3.1. UV/visible spectrophotometric Analysis

The UV-Visible analysis was used initially to verify the effectivepreparation and presence of ZnO NPs. Figure. 2 (A) displays the supreme absorption peak obtained at 378 nm, while Figure. 2 (B) shows the constancy of ZnO NPs that they were steady from new to 60 days. According to the described data,ZnO NPs are confirmed in the 320-390 nm range[23].The authors confirmed the UV absorption spectrum range of ZnO NPs at 376 nm[24] and 380 nm[25].

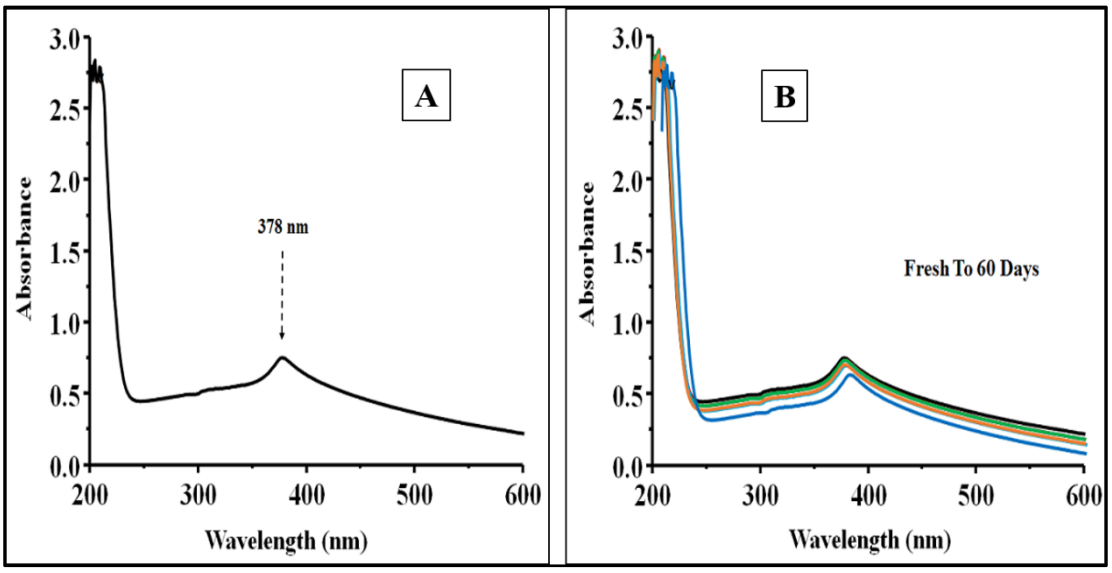

Figure.2: UV-Visible spectra of ZnO NPs.

3.2. Fourier transform-infrared Analysis

In the range of 4000 to 500 cm^{-1}, the FT-IR study was achieved to identify the surface functionality of the ZnOnanomaterials. The typical spectrum shows the interatomic vibrations below 1000 cm^{-1} correspond to ZnO NPs. In Figure. 3the broad absorption band in the range 3400 to 3500 cm^{-1}checks the hydroxyl group stretching vibration which showsthe absorption of water on the surface of ZnO NPs. The highly sharp and intense peak observed in the range of 433 to 510 cm^{-1} correspond to the vibrational stretching of the ZnO NPs indicating the fruitful manufacture of ZnO NPs[26].

Annals of R.S.C.B., ISSN: 1583-6258, Vol. 25, Issue 7, 2021, Pages. 1473 – 1488
Received 05 May 2021; Accepted 01 June 2021.

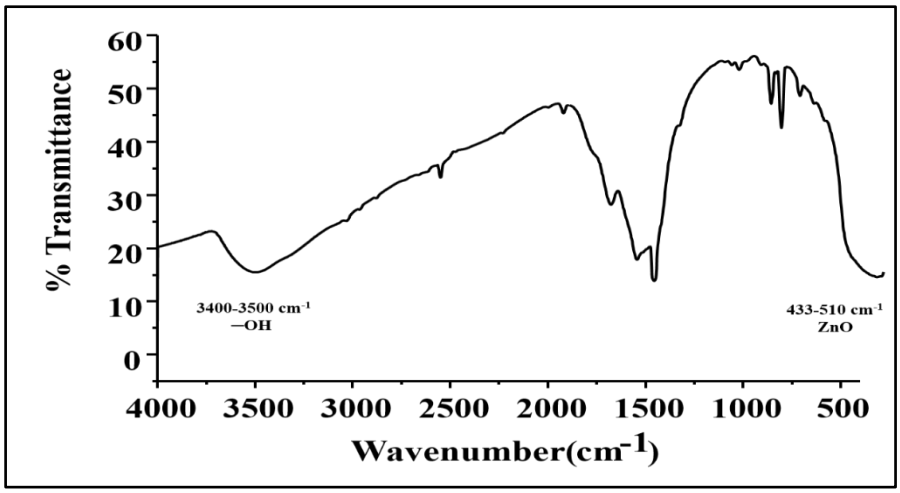

Figure.3: FT-IR Spectra of ZnO NPs.

3.3. Scanning electron microscopic Analysis

SEM analysis was employed to certify the surface topography of engineered ZnONPs, and it was carried out at low and high resolutions. The Figure. 4 displays the cluster shaped morphology having like 13 nm of thickness. It can easily be observed from the image that ZnO NPs are highly scattered showing strong roughness which displays nanomaterial having a great surface to volume ratio and are well-organized as a catalyst in the catalytic reactions[27].

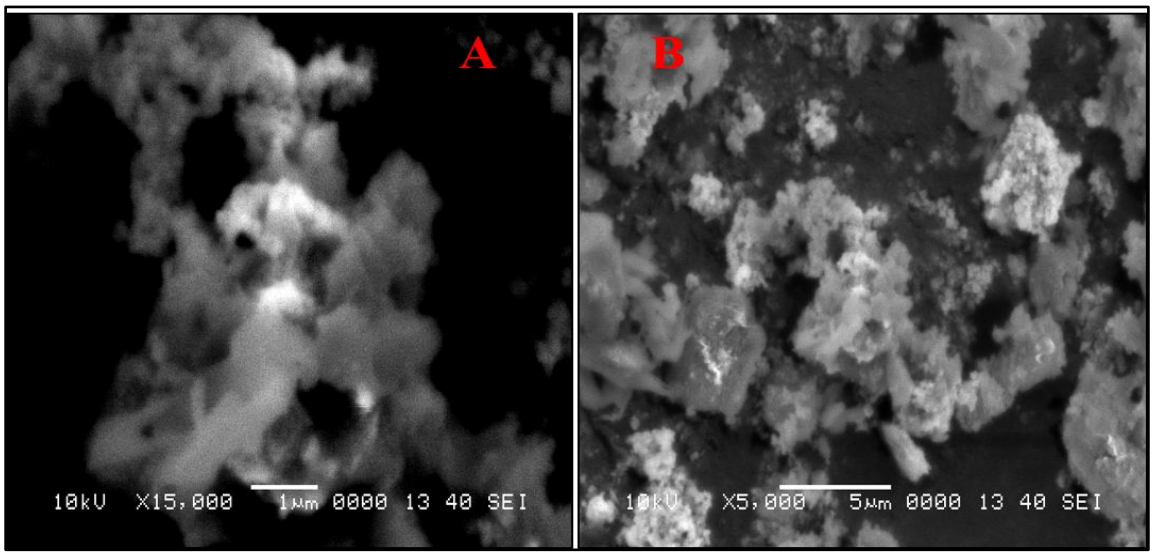

Figure.4: SEM images of ZnO NPs.

3.4. Atomic force microscopic Analysis

The 3-D surface morphology measurement of nanoparticles was investigated via an atomic force microscope (AFM). The AFM investigation reveals the effective fabrication of ZnO NPs via simple and eminent co-precipitation protocol. The usual size of ZnO NPs was measured to be 13 nm, which is evidenced by smaller sized nanostructures and a great match with the size measured from XRD data. As it can be observed in Figure. 5 (A) 2-D image, (B) 3-D image, and (C) particle size distribution, hence nanoparticles are broadlyscattered over a large area with massive irregularity evidenced that the nanostructure could be an excellent postulant in catalytic practicalities[28].

Annals of R.S.C.B., ISSN: 1583-6258, Vol. 25, Issue 7, 2021, Pages. 1473 – 1488
Received 05 May 2021; Accepted 01 June 2021.

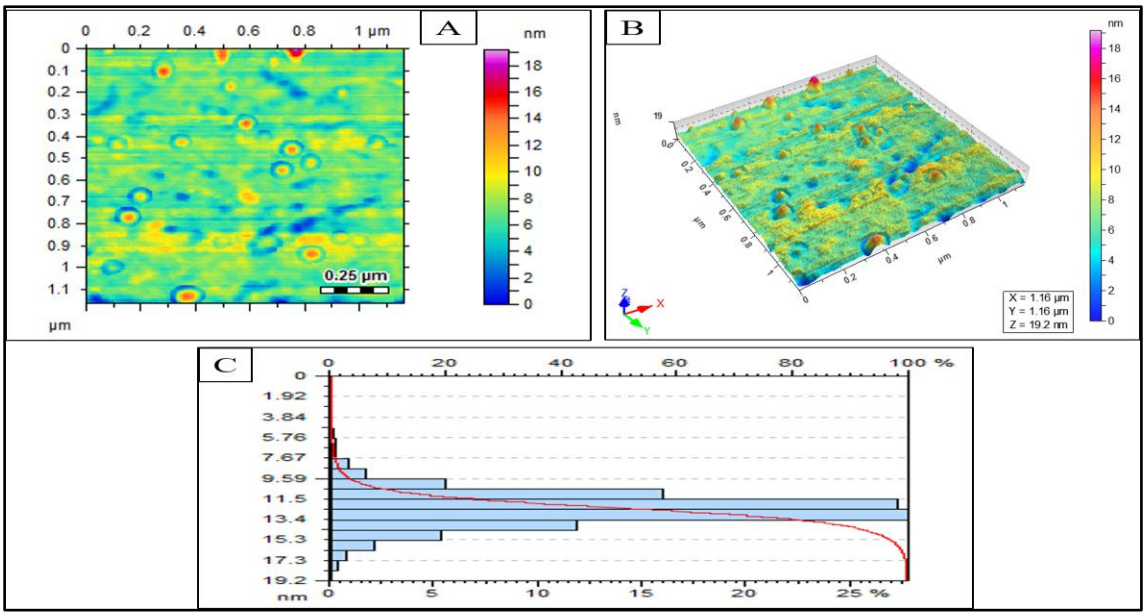

Figure. 5: AFM images of ZnO NPs.

3.5. X-ray diffraction Analysis

The x-ray diffraction (XRD) technique was used to confirm the crystalline nature, phase purity, and average size of the engineered ZnO NPs. It can be seen in Figure. 6, the diffraction plane at (100), (002), (101), (102), (110), (103), (112), and (201) confirms a high degree of crystallinity and wurtzite hexagonal structure of prepared ZnOnanomaterials. Additionally, the Debye Scherrer formula was used to calculated regular crystalline size (13-14 nm) of the preparedZnO NPs using the utmost strong plane in the diffractogram, having formula.

$$D = \frac{k\lambda}{\beta cos\theta} \qquad (2)$$

Here D is the mean crystalline size, K is the dimensionless form feature taken as a continual which has a value of 0.9, lambda (λ) is the wavelength of incident x-ray radiation, β represent the width at the mean peak height and θ is the diffraction angle of ZnO NPs respectively[29].

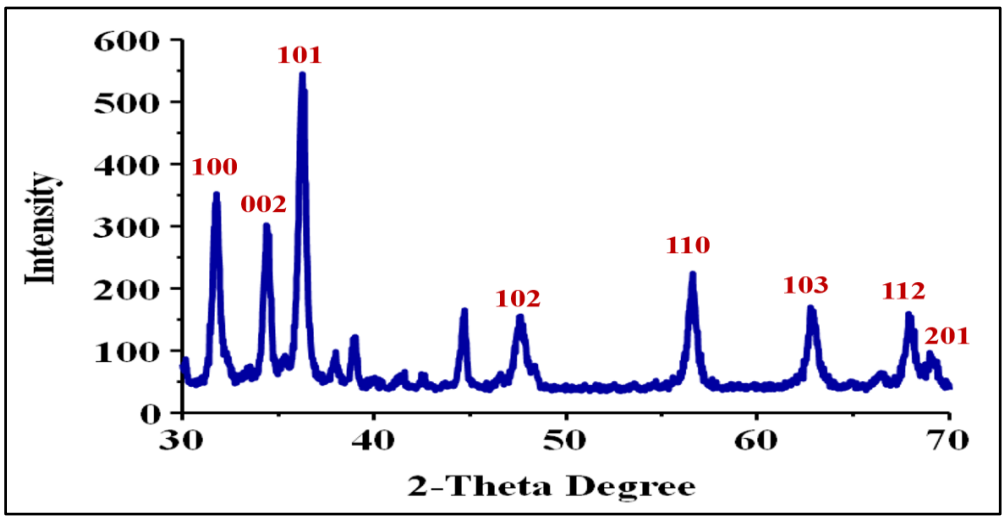

Figure.6: XRD spectra of ZnO NPs.

3.6. Zeta potential analysis

The surface potential was manifested by employing nano zeta seizer as an investigative tool. The Figure. 7 shows a maximum peak of ZnO NPs obtained at -20.0 mV on optimized conditions 0.276

Annals of R.S.C.B., ISSN: 1583-6258, Vol. 25, Issue 7, 2021, Pages. 1473 – 1488
Received 05 May 2021; Accepted 01 June 2021.

conductivity, 100% area, 5.14 mV zeta deviation. The higher zeta potential values of more than 30 mV show the stability of nanoparticles due to a larger electrostatic repulsion between particle results were observed with previously reported work[30].

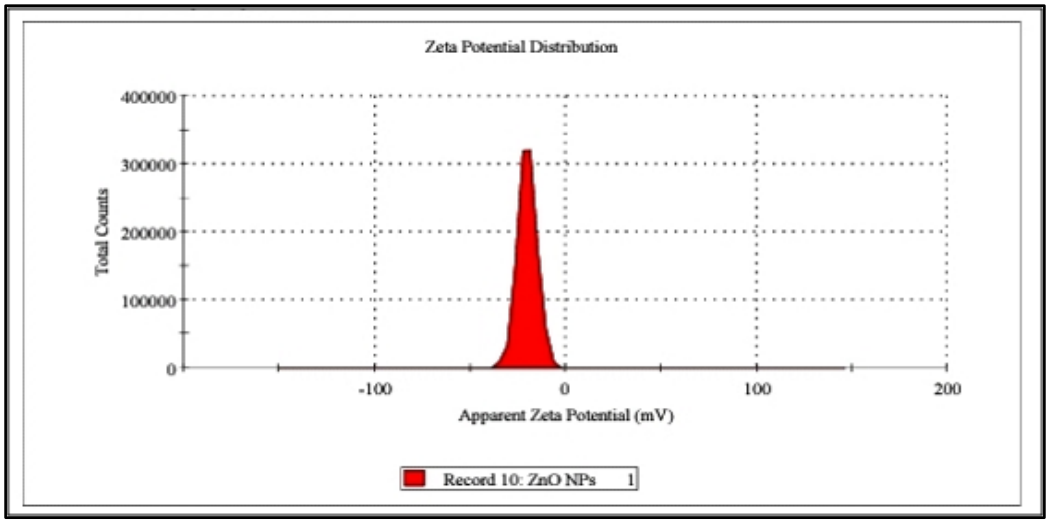

Figure.7: Zeta Potential spectra of ZnO NPs.

4. Catalytic Performance of Synthesized ZnONanocatalyst for the Degradation of Dyes Optimization of Parameters

4.1. Study of pH Effect

The most imperative factor is a pHeffect that helps in the reduction of Rose Bengal (RB) and Eosin Y (EY).To check this effect different solutions of both RB and EY were prepared to have differentpHvalues range from 3-9. Figure. 8 (A-B) shows the maximum % reduction observed near 7 pH, around74, and 72 % reduction was checked in the case of RB and EY respectively using appropriate dyesolution (30 ppm), a reducing agent (50 µL), and catalyst dose (100 µg). The percent reductiongraph is also shown in the inset of the Figureure (A-B) which further confirms the reductionpercentage.

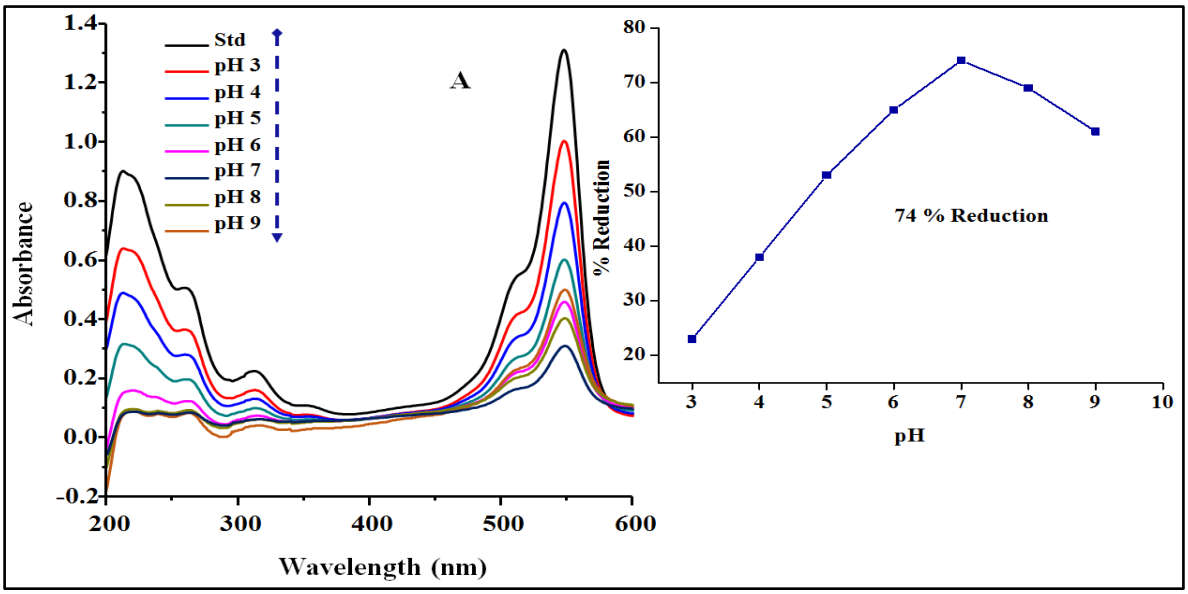

Annals of R.S.C.B., ISSN: 1583-6258, Vol. 25, Issue 7, 2021, Pages. 1473 – 1488
Received 05 May 2021; Accepted 01 June 2021.

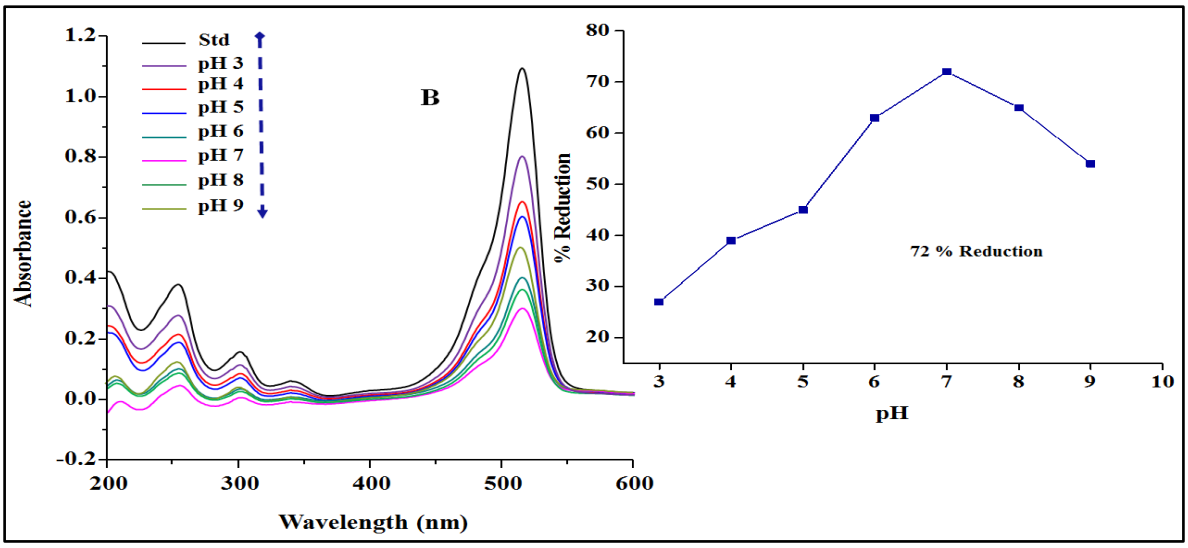

Figure. 8: (A) Effect of pH on RB % reduction (B) Effect of pH on EY % reduction.

4.2. Study of Sunlight Irradiation Time Effect

For both dyes Rose Bengal (RB) and Eosin Y (EY) degradation, sunlight irradiation time isanother key factor to verify its effectiveness various samples of RB and EY 30 ppm of dye solutionwere prepared to have 50 µg catalyst dose and reducing agent near 7 pH and were kept undersunlight for optimization of sunlight effect at regular interval of time. Figure. 9 (A-B) displayedmaximum degradation observed to be 75 and 73 % in the case of RB and EY respectively utilizing30 min of sunlight irradiation. This enhanced performance is due to increased temperature becauseof solar light radiation. It is clear from the Figureure that dye reduces more with increasing sunlightirradiation time. The percent reduction graph is also shown in the inset of the Figureure which furtherconfirms reduction percentages.

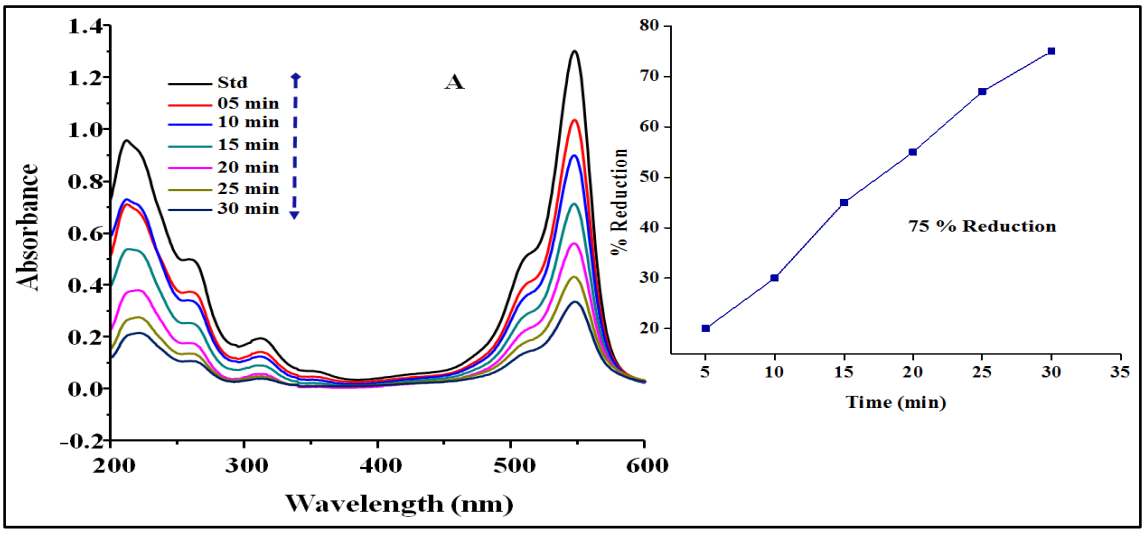

Annals of R.S.C.B., ISSN: 1583-6258, Vol. 25, Issue 7, 2021, Pages. 1473 – 1488
Received 05 May 2021; Accepted 01 June 2021.

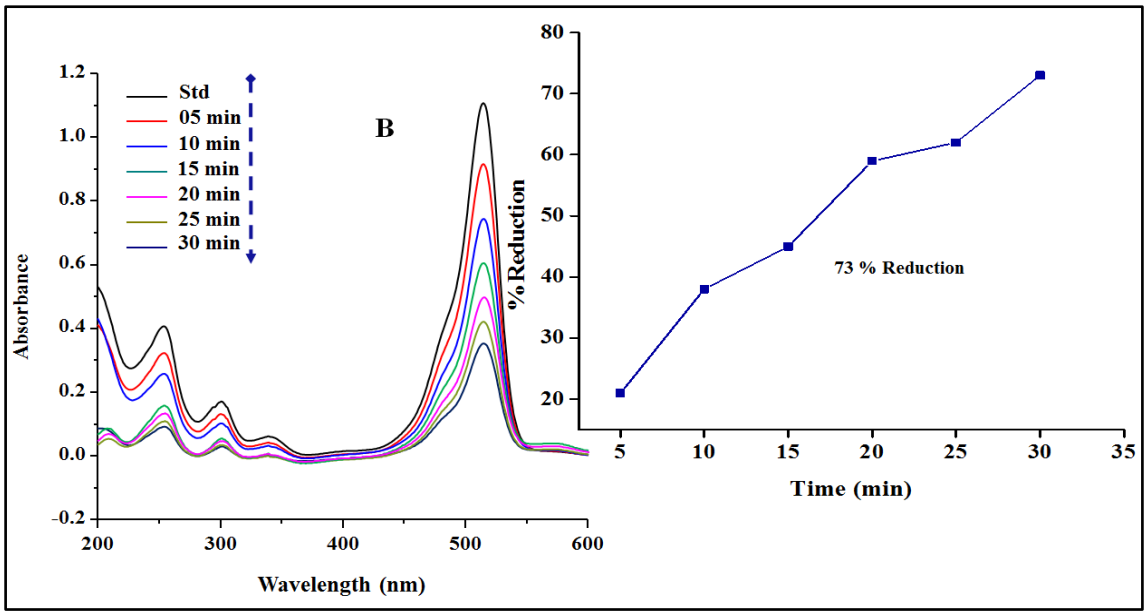

Figure. 9: (A) Effect of sunlight irradiation time on RB % reduction (B) Effect of sunlight irradiation time on EY % reduction.

4.3. Study of Dye Concentration Effect

Thedye concentration effect was checked to validate the volume of dye consumed to checkthe trace level reduction of Rose Bengal (RB) and Eosin Y (EY). In this effect, differentconcentrations (i.e. 60, 50, 40, 30, 20, 10 ppm) of RB and EY dye solution were prepared, fromeach concentration appropriate volume was taken having 50 µg catalyst dose and reducing agentat 7 pH. It is clear from Figure. 10 (A-B) reveals maximum reduction percentage observed to be 79and 76 % for RB and EY respectively. The percent reduction graph is also shown in the inset ofthe Figureure which further confirms the reduction percentage.

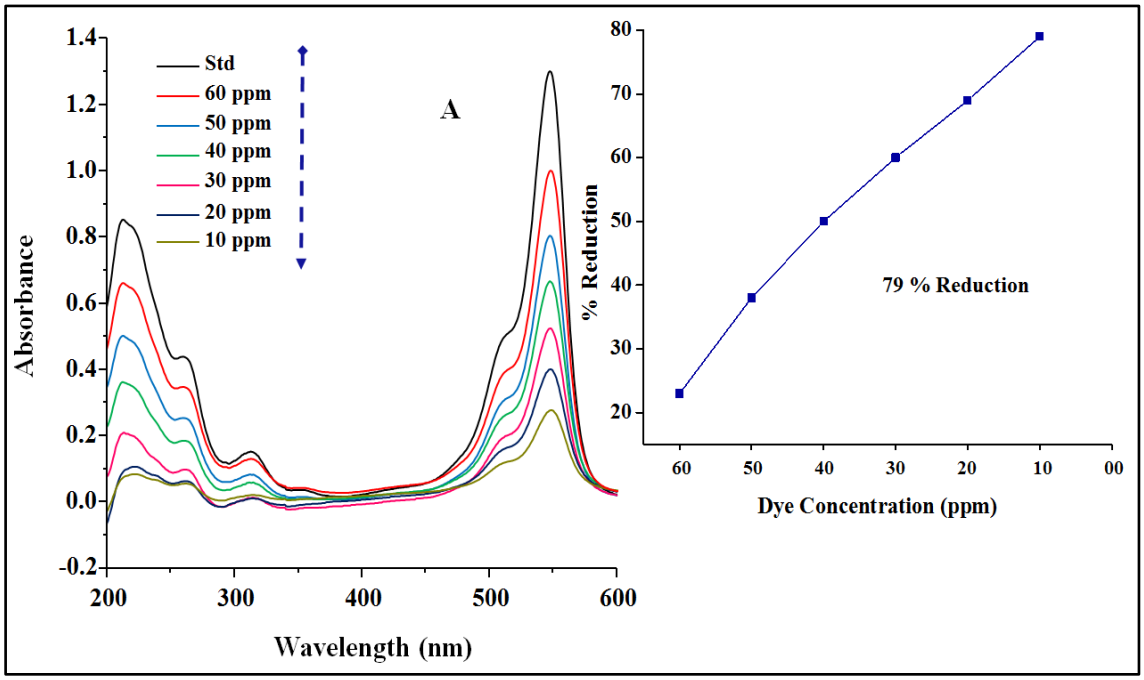

Annals of R.S.C.B., ISSN: 1583-6258, Vol. 25, Issue 7, 2021, Pages. 1473 – 1488
Received 05 May 2021; Accepted 01 June 2021.

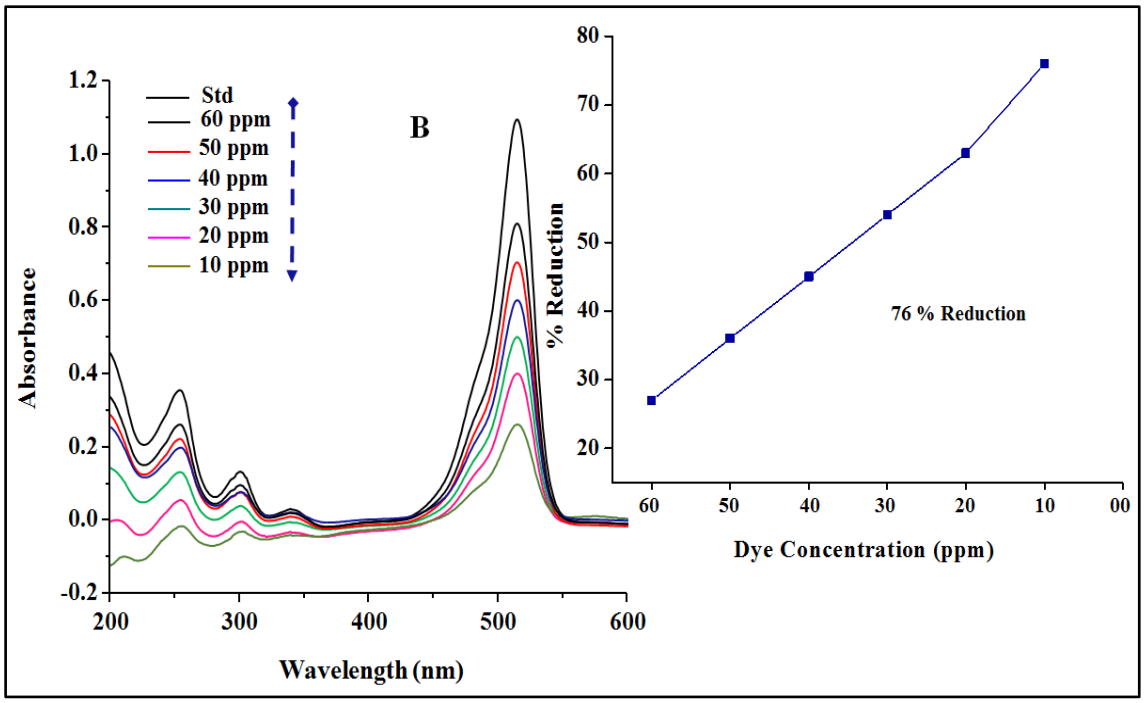

Figure. 10: (A) Effect of dye concentration on RB % reduction (B) Effect of dye concentration on EY % reduction.

4.4. Study of Catalyst Dose in the absence of Reducing Agent Effect

The effectiveness of the preparednanocatalyst is assessed to recognize the importance through theoptimization of catalyst dose. To evaluate this step appropriate volume of 30 ppm Rose Bengal(RB) and Eosin Y (EY) solution was taken in a test tube along with 50-300 and 100-350 µgof catalyst dose respectively, following optimized pH (7) by utilizing 3 min then spectra wererecorded. As it is clear from Figure. 11 (A-B) maximum reduction was observed to be 85 and 80 %in the case of RB and EY, respectively. The percent reduction graph is also shown in the inset ofthe Figureure which further confirms the reduction percentage.

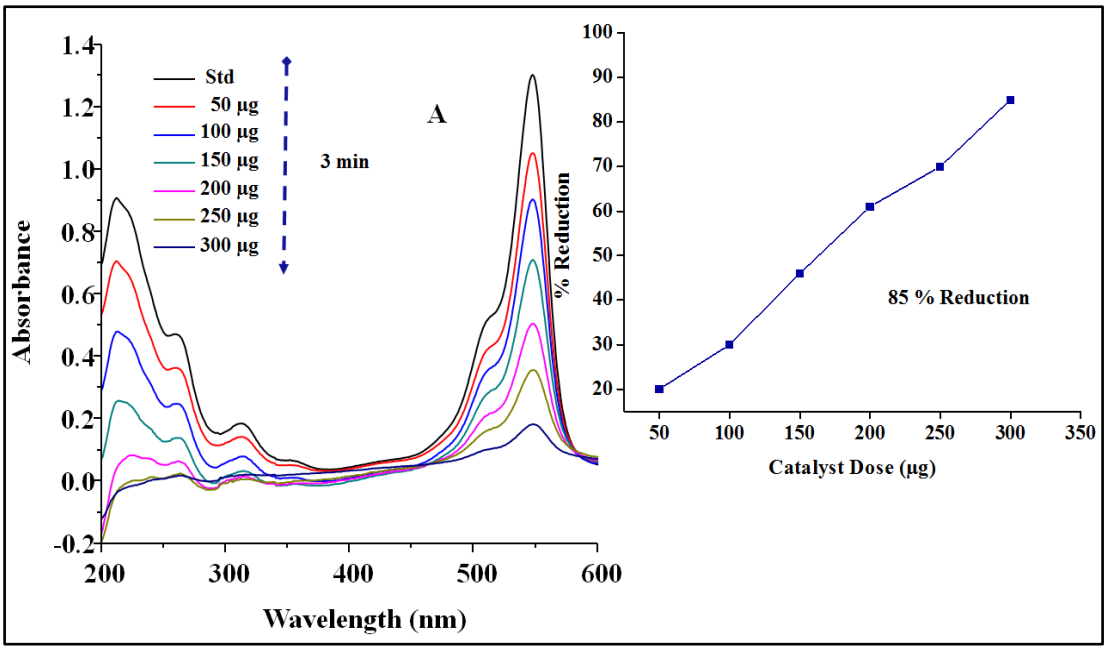

Annals of R.S.C.B., ISSN: 1583-6258, Vol. 25, Issue 7, 2021, Pages. 1473 – 1488
Received 05 May 2021; Accepted 01 June 2021.

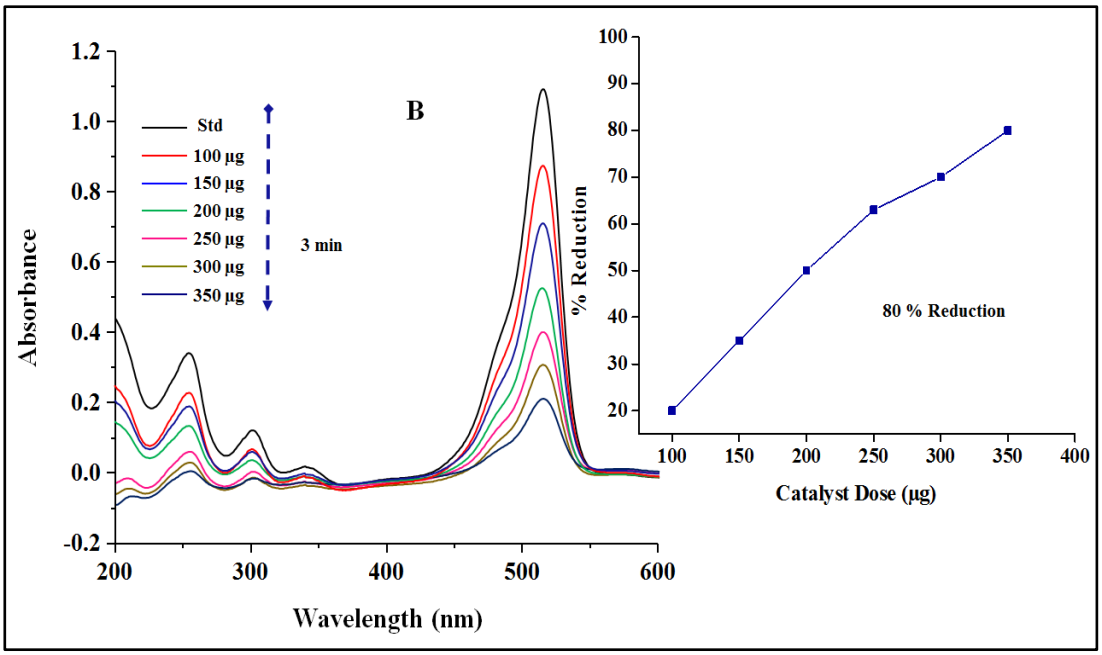

Figure. 11: (A) Effect of catalyst dose in the absence of reducing agent on RB % reduction (B) Effect of catalyst dose in the absence of reducing agent on EY % reduction.

4.5. Study of Catalyst Dose in the presence of Reducing Agent Effect

The effectiveness of the preparednanocatalyst is estimated to identifythe importance ofapplying instantproton source from $NaBH_4$. To make the work worthwhile various factors were optimized such aspH, dye concentration, solar light irradiation, and catalyst dose hence reducing agent needs to beoptimized to add further efficacy of nanocatalyst. In this step, the volume of $NaBH_4$was optimizedin the range of 50-300 and 100- 350 µL RB and EY respectively by utilizing 3 min then spectrawere obtained. As it is clear from Figure. 12 (A-B) maximum reduction was observed to be 98 and95 % in the case of RB and EY, respectively. The percent reduction graph is also shown in the insetof the Figureure which further confirms the reduction percentage.

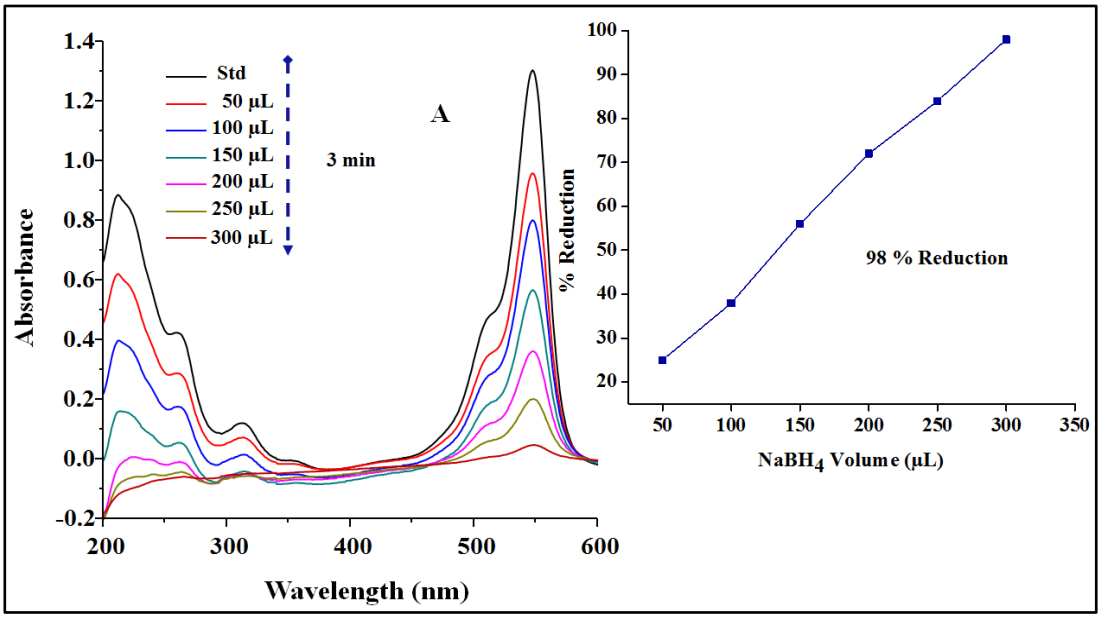

Annals of R.S.C.B., ISSN: 1583-6258, Vol. 25, Issue 7, 2021, Pages. 1473 – 1488
Received 05 May 2021; Accepted 01 June 2021.

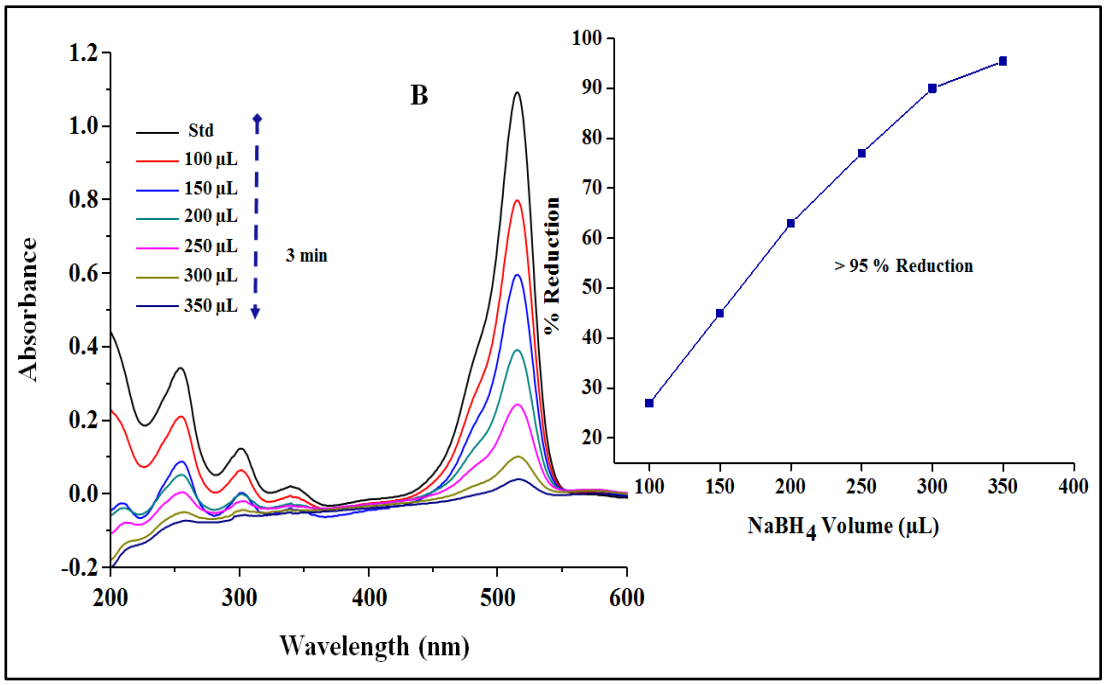

Figure. 12: (A) Effect of catalyst dose in the presence of reducing agent on RB % reduction (B) Effect of catalyst dose in the presence of reducing agent on EY % reduction.

5. Mechanism of Degradation of Dyes

In themechanism of degradation of the dyes, the creation of a hole in the valence band is shaped simultaneously electron is excited to conduction band from the valence band on the action of ZnO NPs withsolar light. These solar-produced hole pairs of electrons can be combined again or interrelate separatelywith other particles. The produced holes can react with H_2O over the catalyst surface resulting •OHwhereas superoxide radical anions are formed by accepting electrons via adsorbed oxygen.Finally, the oxidized product was obtained by the treatment of dye with hydroxyl radicals(powerful oxidizing agent)as shown in Figure. 13. The whole stepwise mechanism is summarizedbelow:

$ZnO + h\nu \rightarrow h^+ + e^-$ (3)

$h^+ + e^- \rightarrow$ heat (4)

$h^+ + H_2O \rightarrow {}^{\bullet}OH + H^+$ (5)

$e^- + O_2 \rightarrow O_2^{\bullet-}$ (6)

$O_2^{\bullet-} + H_2O \rightarrow H_2O_2 \rightarrow 2{}^{\bullet}OH$ (7)

${}^{\bullet}OH$ + dyes → Oxidized product (8)

Annals of R.S.C.B., ISSN: 1583-6258, Vol. 25, Issue 7, 2021, Pages. 1473 – 1488
Received 05 May 2021; Accepted 01 June 2021.

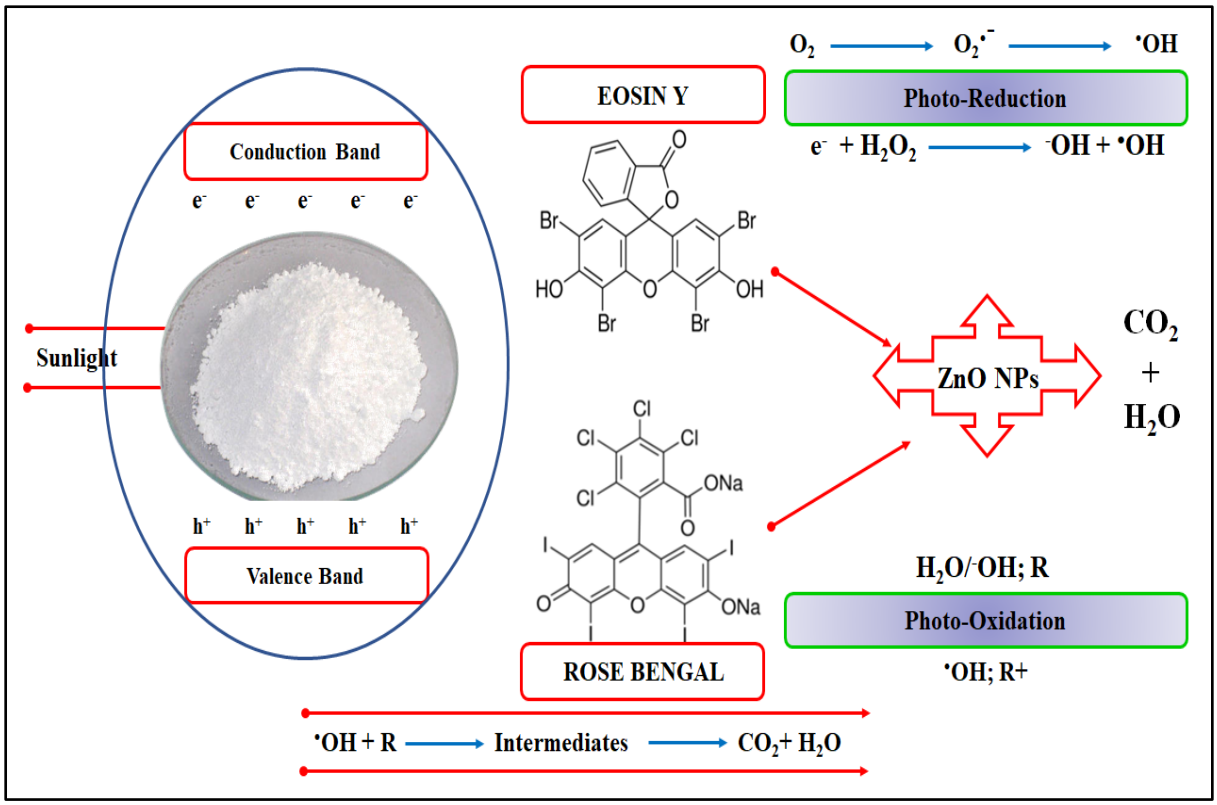

Figure. 13: Mechanism of degradation of RB and EY dyes.

6. Comparative Study

ZnO NPs are highly active for the degradation of dyes as compared to previously reported work,hence among several metal oxide nanoparticles, this work is more superior to all reported work dueto its better % reduction, a small amount of catalyst, less time consuming, etc.

Table no 1 Comparison the Results of Rose Bengal with Previously Reported Work

Material	Illumination Source	Catalyst Dose (g)	Time (min)	(%) Degradation	Ref
γ-Fe2O3	Visible light	0.625	210	~98	[31]
SnO_2	Sunlight	0.20	90	78-96	[32]
NF1	Sunlight	0.20	60	86	[33]
ZnO	**Sunlight**	**3×10^{-4}**	**3**	**98.7**	**PresentWork**

Table no 2 Comparison the Results of Eosin Y with Previously Reported Work

Material	Illumination Source	Catalyst Dose (g)	Time (min)	(%) Degradation	Ref
$Fe_2Mo_3O_{12}$	Visible light	100×10^{-3}	120	96.6	[34]

Annals of R.S.C.B., ISSN: 1583-6258, Vol. 25, Issue 7, 2021, Pages. 1473 – 1488
Received 05 May 2021; Accepted 01 June 2021.

AG-Au	UV light	5×10^{-3}	180	83	[35]
Hes-TiO_2	Visible light	0.375	180	96	[36]
ZnO	**Sunlight**	**3.5×10^{-4}**	**3**	**≥ 95**	**PresentWork**

7. Reusability of Nanocatalyst

The study was carried out to identify the effectiveness of the ZnOnanocatalystreusage as shown in Figure. 14 the engineered ZnOnanocatalyst found great potential towards the degradation of toxic dyes for several intervals. The particles were filtered and dried at atmospheric temperature. The cycle was repeated five times, 95% EY, and 98% RB was degraded in 1stseries which gradually decrease per cycle as 88%, 80%, 74%, and 68% for 2nd, 3rd, 4th, and 5thcycles, respectively.

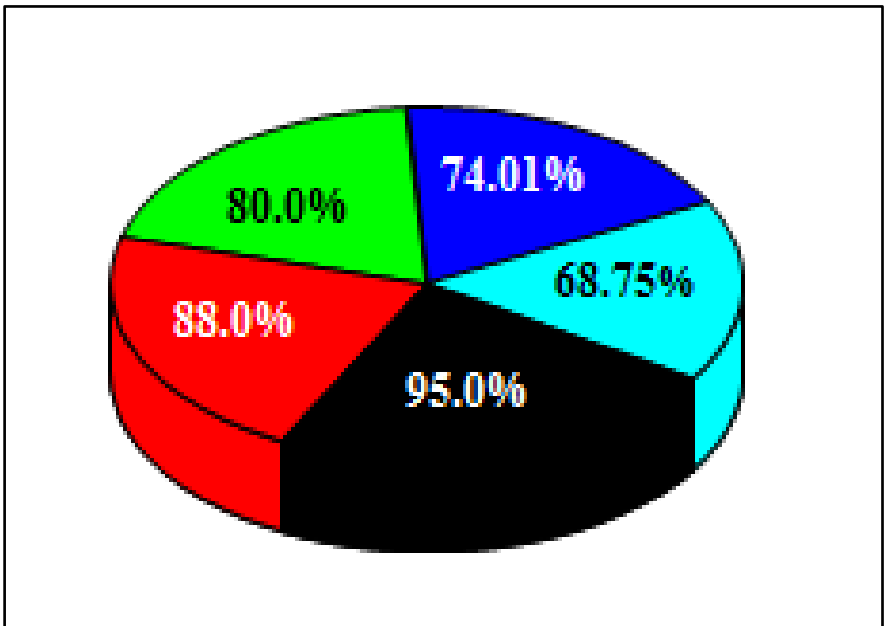

Figure. 14: Reusability of ZnO NPs.

8. Conclusion

ZnO NPs were prepared by applying a simple and easy co-precipitation procedureand subjected tovarious techniques for characterization to confirm the formation of nanostructures.The size, shape, and morphological characteristics were determined by AFM, XRD, and SEM. The data revealsthe size of 13.4 nm of particles with the wurtzite hexagonal crystallinephase and clusters morphology. Whereas the charge on nanoparticles was monitored by zetapotential that discloses an excellent charge of (-20.0 mV) over their surface. High photocatalyticefficiency for the degradation of dyes up to 98% was observed. Consequentially,ZnO NPs can be suggested as a well-organizedphotocatalyst for the successful degradation of toxiccomplexeddyes for the aquatic environment at the commercial level.

References

[1] T. Robinson, G. McMullan, R. Marchant and P. Nigam, Bioresource technology, **77,** 247-255, (2001).

Annals of R.S.C.B., ISSN: 1583-6258, Vol. 25, Issue 7, 2021, Pages. 1473 – 1488
Received 05 May 2021; Accepted 01 June 2021.

[2] A. Savk, B. Sen, B. Demirkan, E. Kuyuldar, A. Aygun, M. S. Nas and F. Sen, Chitosan-Based Adsorbents Wastewater Treat, **45,** 57-80, (2018).
[3] F. Chen, X. Wu, R. Bu and F. Yang, RSC advances, **7,** 41945-41954, (2017).
[4] V. Rajagopalan, Scientific reports, **6,** 1-10, (2016).
[5] H. Fu, C. Pan, W. Yao and Y. Zhu, The Journal of Physical Chemistry B, **109,** 22432-22439, (2005).
[6] A. Ajmal, I. Majeed, R. N. Malik, H. Idriss and M. A. Nadeem, RSC advances, **4,** 37003-37026, (2014).
[7] A. Molla, M. Sahu and S. Hussain, Journal of Materials Chemistry A, **3,** 15616-15625, (2015).
[8] H. R. Pouretedal, A. Norozi, M. H. Keshavarz and A. Semnani, Journal of Hazardous Materials, **162,** 674-681, (2009).
[9] R. Jeyachitra, V. Senthilnathan and T. Senthil, Journal of Materials Science: Materials in Electronics, **29,** 1189-1197, (2018).
[10] A. H. Pato, A. Balouch, F. N. Talpur, A. M. Mahar, M. T. Shah, A. Kumar, S. Qasim and A. A. Gabole, Applied Nanoscience, **10,** 739-749, (2020).
[11] A. M. Mahar, A. Balouch, F. N. Talpur, P. Panah, R. Kumar, A. Kumar, A. H. Pato, D. Mal, S. Kumar and A. A. Umar, Environmental Science and Pollution Research, **54,** 1-9, (2020).
[12] A. Fujishima and K. Honda, nature, **238,** 37-38, (1972).
[13] Y.-K. Lai, J.-Y. Huang, H.-F. Zhang, V.-P. Subramaniam, Y.-X. Tang, D.-G. Gong, L. Sundar, L. Sun, Z. Chen and C.-J. Lin, Journal of Hazardous Materials, **184,** 855-863, (2010).
[14] C. Xu, G. Rangaiah and X. Zhao, Industrial & Engineering Chemistry Research, **53,** 14641-14649, (2014).
[15] X. Wang, J. Gao, B. Xu, T. Hua and H. Xia, RSC advances, **5,** 87233-87240, (2015).
[16] X. Niu, H. Li and G. Liu, Journal of Molecular Catalysis A: Chemical, **232,** 89-93, (2005).
[17] J. Kaur and S. Singhal, Physica B: Condensed Matter, **450,** 49-53, (2014).
[18] A. Mittal, D. Jhare and J. Mittal, Journal of Molecular Liquids, **179,** 133-140, (2013).
[19] S. Sharma, R. P. Goyal, G. Chakravarty and A. Sharma, Experimental and Toxicologic Pathology, **60,** 51-57, (2008).
[20] M. Anjum, R. Miandad, M. Waqas, F. Gehany and M. Barakat, Arabian Journal of Chemistry, **12,** 4897-4919, (2019).
[21] L. Wang, J. Li, Y. Wang, L. Zhao and Q. Jiang, Chemical Engineering Journal, **181,** 72-79, (2012).
[22] J. Ali, R. Irshad, B. Li, K. Tahir, A. Ahmad, M. Shakeel, N. U. Khan and Z. U. H. Khan, Journal of Photochemistry and Photobiology B: Biology, **183,** 349-356, (2018).
[23] P. Jamdagni, P. Khatri and J. Rana, Journal of King Saud University-Science, **30,** 168-175, (2018).
[24] A. Raja, S. Ashokkumar, R. P. Marthandam, J. Jayachandiran, C. P. Khatiwada, K. Kaviyarasu, R. G. Raman and M. Swaminathan, Journal of Photochemistry and Photobiology B: Biology, **181,** 53-58, (2018).
[25] J. Santhoshkumar, S. V. Kumar and S. Rajeshkumar, Resource-Efficient Technologies, **3,** 459-465, (2017).
[26] A. R. West, John Wiley & Sons, **70,** (2014).

Annals of R.S.C.B., ISSN: 1583-6258, Vol. 25, Issue 7, 2021, Pages. 1473 – 1488
Received 05 May 2021; Accepted 01 June 2021.

[27] A. Askarinejad, M. A. Alavi and A. Morsali, Iranian Journal of Chemistry and Chemical Engineering (IJCCE), **30,** 75-81, (2011).
[28] S. Nagarajan and K. A. Kuppusamy, Journal of nanobiotechnology, **11,** 39, (2013).
[29] S. Getie, A. Belay, A. Chandra Reddy and Z. Belay, J. Nanomed. Nanotechnol. S, **8,** 004, (2017).
[30] R. Marsalek, APCBEE procedia, **9,** 13-17, (2014).
[31] A. K. Dutta, S. K. Maji and B. Adhikary, Materials Research Bulletin, **49,** 28-34, (2014).
[32] R. Malik, V. K. Tomer, P. S. Rana, S. Nehra and S. Duhan, Materials Letters, **154,** 124-127, (2015).
[33] A. Khatri and P. S. Rana, Physica B: Condensed Matter, **579,** 411905, (2020).
[34] P. Suresh, U. S. Kumari, T. S. Rao and A. P. Rao, J. Aplicble. Chem, **3,** 2047-2054, (2014).
[35] M. Chokkalingam, E. J. Rupa, Y. Huo, R. Mathiyalagan, G. Anandapadmanaban, J. C. Ahn, J. K. Park, J. Lu and D. C. Yang, Optik, **185,** 1213-1219, (2019).
[36] K. Vignesh, A. Suganthi, M. Rajarajan and R. Sakthivadivel, Applied surface science, **258,**4592-4600, (2012).